Available online at www.sciencedirect.com
SCIENCE DIRECT®
PERGAMON
International Journal of Multiphase Flow 29 (2003) 1249–1263
International Journal of Multiphase Flow
www.elsevier.com/locate/ijmulflow

Performance evaluation of a low-temperature waste heat driven multi-bed adsorption chiller

B.B. Saha [a,*], S. Koyama [a], J.B. Lee [b], K. Kuwahara [a], K.C.A. Alam [c], Y. Hamamoto [c], A. Akisawa [c], T. Kashiwagi [c]

[a] *Institute for Materials Chemistry and Engineering, Kyushu University, 6-1 Kasuga-koen, Kasuga-shi, Fukuoka 816-8580, Japan*
[b] *Division of Mechanical and Automation Engineering, Kyungnam University, 449 Wolyoung-dong, Masan, Kyungnam 631-701, South Korea*
[c] *Bio-Applications and Systems Engineering, Tokyo University of Agriculture & Technology, 2-24-16 Naka-machi, Koganei-shi, Tokyo 184-8588, Japan*

Received 25 October 2002; received in revised form 20 May 2003

Abstract

This study aims at improving the performance of thermally activated silica gel–water adsorption refrigeration cycle by applying multi-bed scheme. In this paper, a three-bed non-regenerative silica gel–water adsorption chiller design is outlined along with the performance evaluation of the innovative chiller. The three-bed chiller will be able to work as high efficient single-stage adsorption chiller where driving source temperature is between 60 and 95 °C along with a coolant at 30 °C. The three-bed cycle comprises with three adsorber/desorber heat exchangers, one evaporator and one condenser. Waste heat or renewable energy sources will power the high temperature desorber. If two beds are in desorption mode, the hot water outlet from the lead desorber will drive the lag desorber before being released to ambient. This facilitates the maximum utilization of the waste stream. On the contrary, if two adsorber or desorber beds are in adsorption mode, the cooling water outlet from the lead adsorber will cool down the lag adsorber. In this circumstance, two adsorber beds will be connected with the evaporator and will enhance evaporation.

A cycle simulation computer program is developed to analyze the influence of operating temperatures (hot and cooling water temperatures, adsorption/desorption cycle time) on cooling capacity and coefficient of performance (COP) of the innovative three-bed cycle in parallel flow configuration of the heat transfer fluids. The cycle simulation calculation indicates that the COP value of the three-bed chiller is 0.38 with a driving source temperature at 80 °C in combination with coolant inlet and chilled water inlet temperatures at 30 and 14 °C, respectively. The delivered chilled water temperature is about 6 °C with this operation condition. Simulation results also show that from the two to three beds, waste heat recovery efficiency, η is boosted by about 35%.

* Corresponding author. Tel.: +81-92-583-7832; fax: +81-92-583-7833.
E-mail address: bidyutb@cm.kyushu-u.ac.jp (B.B. Saha).

0301-9322/03/$ - see front matter © 2003 Elsevier Ltd. All rights reserved.
doi:10.1016/S0301-9322(03)00103-4

Keywords: Adsorption; Chiller; Multi-bed; Refrigeration; Waste heat recovery

1. Introduction

Over the past three decades there have been considerable efforts to use adsorption (solid/vapor) for cooling and heat pump applications, but intensified efforts were initiated only since the imposition of international restrictions on the production and use of CFCs (chlorofluorocarbons) and HCFCs (hydrochloroflurocarbons). A considerable number of studies have been conducted on solid–vapor heat pump systems. The followings are some representative examples.

Tchernev (1979) studied a solid–vapor system using the zeolite–water pair for solar air conditioning and refrigeration. The same adsorbent–refrigerant pair was studied by Alefeld et al. (1981) for heat pump and heat storage application. Zeolite composites and water cycles were investigated by Guilleminot et al. (1994). The composites they used are (a) 65% zeolite + 35% metallic foam and (b) 70% zeolite + 30% natural expanded graphite.

Pons and Guilleminot (1986), and Exell et al. (1993) studied the activated carbon–methanol system for ice production by using renewable energy. Tamainot-Telto and Critoph (2001) suggested the utilization of monolithic carbon as adsorbent for refrigeration and heat pump applications.

Beijer and Horsman (1994) studied the complex compound/salts adsorption cycle for vehicles and residential air conditioning.

The silica gel–water system was investigated analytically by Saha et al. (1995), Chua et al. (1999) and experimentally by Boelman et al. (1995) for adsorption cooling by using waste heat as the driving source.

All the above mentioned cycles are basic cycles. Advanced cycles are usually designed to attain higher performance. Douss and Meunier (1989) proposed and analyzed a cascading adsorption cycle in which an active carbon–methanol cycle is topped by a zeolite–water cycle. The experimental COP reaches 1.06 with driving heat source around 250 °C.

Klein et al. (2000) investigated two different combinations of coupling cycles. In the first combination, a metal hydride single stage cycle is topped by a zeolite–water cycle. While in the second combination a silica gel–water cycle is topped with a double-stage metal hydride cycle. The overall COP values are 1.53 and 1.55 respectively, for the first and second combinations.

Waste heat driven silica gel–water based two-bed adsorption chillers have been successfully commercialized in Japan. For a conventional adsorption chiller, the lowest regeneration temperature has been reached at 60 °C in combination with a coolant at 30 °C. Even lower driving source temperature, in the range of 40 °C with similar coolant temperature, has been experimentally proven to be viable for a three-stage adsorption chiller by Saha and Kashiwagi (1997). These examples show that silica gel–water adsorption chiller is well suited to low-temperature waste heat utilization for producing effective cooling power. However, the drawback of multi-stage adsorption system is its poor performance and fluctuation in delivered chilled water temperature.

In order to improve the recovery efficiency of waste heat to useful cooling and reduce the chilled water outlet temperature fluctuation, a four-bed regenerative scheme is proposed and its per-

formance was solved numerically by Chua et al. (2001). The waste heat recovery efficiency of the four-bed regenerative chiller is about 70% higher than that of the conventional chiller. The drawbacks are the requirement of two more sorption elements, which results in higher initial cost.

In this paper, a three-bed non-regenerative silica gel–water adsorption chiller design is proposed. A cycle simulation computer program of the innovative three-bed chiller is developed to analyze the cooling capacity and COP variations by varying heat transfer fluid (hot and cooling water) inlet temperatures and adsorption/desorption cycle time along with the effect driving source temperatures on waste heat recovery efficiency.

2. Working principle of the three-bed adsorption cycle

The proposed three-bed strategy is an extension from the conventional (two-bed) operation. In a conventional adsorption chiller, the inherent restriction in the number of beds resulted in significant temperature fluctuation at all the components. The peak temperature of the condenser outlet that follows shortly after the bed switching adds on to the instantaneous load of the cooling tower. The three-bed scheme will serve to reduce the peak temperatures in both the evaporator and condenser.

Fig. 1(a) and Table 1 depict the schematic diagram and time allocation scheme of the three-bed adsorption cycle, respectively, in parallel flow configuration. The three-bed cycle comprises with an evaporator, a condenser and three sorption elements (adsorber/desorber heat exchangers). Refrigerant (water), evaporates inside the evaporator, picking up evaporation heat from the chilled water, is adsorbed by adsorber 1 (SE1) via valve 1 as can be seen from Fig. 1(a).

The adsorption of water vapor into silica gel results in the release of adsorption heat. Accordingly, the temperature of the SE1 during adsorption mode rises, which reduces its water vapor uptake capacity. Cooling water removes adsorption heat from the SE1. As can be seen from Fig. 1(a), SE2 is disconnected with either evaporator or condenser by closing valves 2 and 5. SE2 is in the pre-heating/pre-cooling mode. Desorber 3 (SE3) is connected to the condenser via valve 6. The desorbed refrigerant vapor is condensed in the condenser at temperature T_{cond}; cooling water removes the condensation heat. The condensed refrigerant comes back to the evaporator via the capillary tube connecting the condenser and evaporator to complete the cycle. The capillary tube is bent for achieving a pressure drop resulting in the refrigerant being in liquid phase inside the evaporator. This will minimize the requirement of super cooling of the incoming refrigerant from condenser. The use of parallel cooling water circuits for the condenser and adsorber 1 results in similar temperature levels at the condenser (T_{cond}) and the adsorber (T_{ads}). When refrigerant concentrations in the adsorber(s) and desorber(s) are at or near their equilibrium level, the flows of hot and cooling water are redirected by switching the valves so that the desorber(s) switch into adsorption mode(s) and the adsorber(s) change into desorption operation(s). This is needed to pre-heat the adsorber(s) and pre-cool the desorber(s). The resulting low-pressure refrigerant is again adsorbed by the adsorbent to continue the process. The energy utilization scheme and operating conditions of the three-bed adsorption chiller are shown in Tables 2 and 3, respectively.

The schematic of the innovative three-bed chiller in series flow configuration is shown in Fig. 1(b). In this mode, by capitalizing the phase difference between the three sorption elements, the heat source from the lead desorber can be used to regenerate another cooler desorber that will act

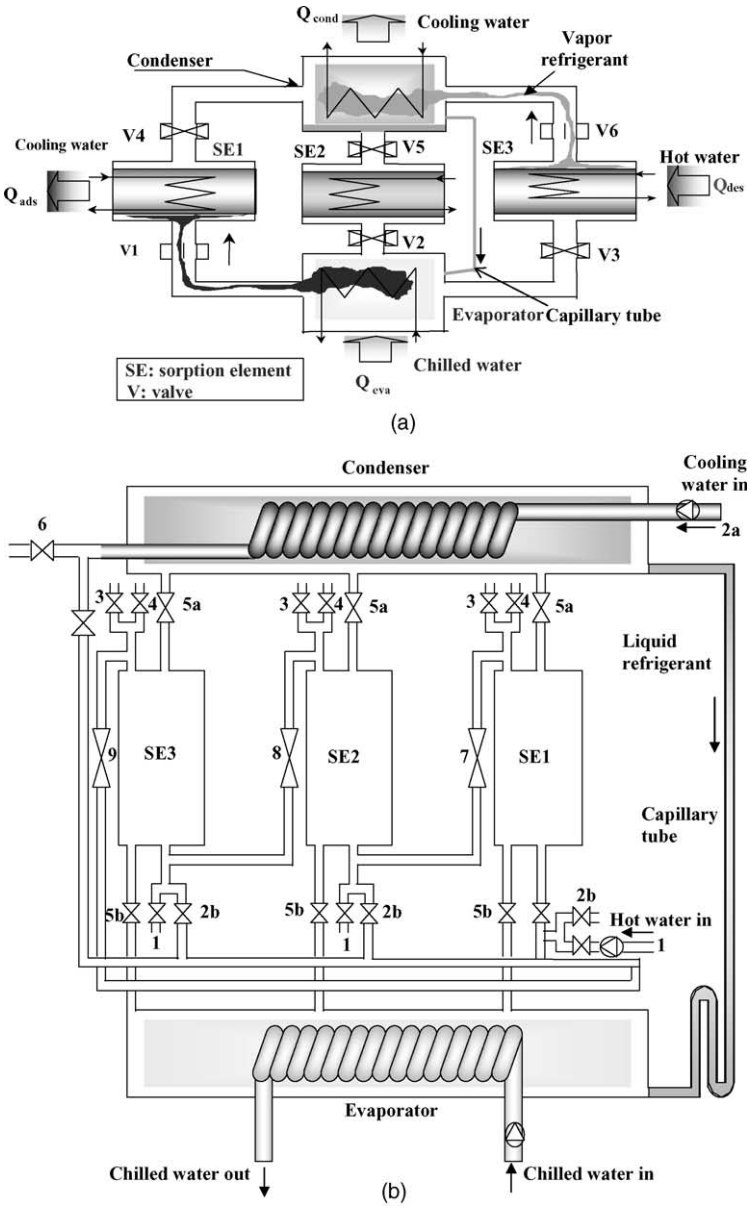

SE: sorption element, **1**: hot water inlet, **2a**: coolant inlet to the condenser, **2b**: coolant inlet to the adsorber, **3**: hot water outlet, **4**: coolant outlet from the adsorber, **5a**: SE connection valve with condenser, **5b**: SE connection valve with evaporator and **6**: coolant outlet from the condenser.

Fig. 1. Schematic diagram of the innovative three-bed adsorption chiller in (a) parallel flow configuration and (b) series flow configuration.

as the lack desorber. The outlet hot water from the lack desorber will be discharged to ambient. Similarly, the coolant from the sorption element(s) in adsorption mode can be used in cascaded

Table 1
Operation mode and time allocation of each sorption element in three-bed adsorption chiller

Sorption element	Operation mode			
	Desorption mode (s) HTF: hot water	Pre-cooling mode (s) HTF: cooling water	Adsorption mode (s) HTF: cooling water	Pre-heating mode (s) HTF: hot water
(a) Total cycle time: 660 s (standard cycle)				
SE1	1–300	301–330	331–630	631–660
SE2	201–500	501–530	1–170, 531–660	171–200
SE3	1–100, 461–660	101–130	131–430	431–460
(b) Total cycle time: 360 s (short cycle)				
SE1	1–150	151–180	181–330	331–360
SE2	101–250	251–280	1–70, 281–360	71–100
SE3	1–50, 261–360	51–80	81–230	231–260
(c) Total cycle time: 1800 s (long cycle)				
SE1	1–870	871–900	901–1770	1771–1800
SE2	381–1250	1251–1280	1–350, 1281–1800	351–380
SE3	1–290, 1221–1800	291–320	321–1190	1191–1220

HTF: heat transfer fluid.

Table 2
Energy utilization scheme for the three-bed adsorption cycle

SE 1	Ads (1)	Sw	Des (1)	Sw
SE 2	Des (1)	Sw	Ads (1)	Sw
SE 3	Ads (1)	Sw	Des (1)	Sw

Ads: adsorber; Des: desorber.
Sw: switching from adsorber to desorber, and receiving heating stream from heat source or switching from desorber to adsorber, and receiving cooling stream directly from the coolant source (1): this refers to the situation when the bed acts as the leading adsorber/desorber. The bed receives either cooling stream directly from the coolant source; or heating stream directly from the heat source.

Table 3
Operating conditions

Parameter	Range (rated condition)
Coolant inlet temperature	20–40 °C (30 °C)
Coolant flow rate (each adsorber)	0.192 kg/s
Coolant flow rate (condenser)	0.332 kg/s
Hot water inlet temperature	60–95 °C (80 °C)
Hot water flow rate (each desorber)	0.191 kg/s
Chilled water inlet temperature	14 °C
Chilled water flow rate	0.0518 kg/s
Adsorption/desorption cycle time	300 s
Pre-heating/pre-cooling cycle time	30 s

manner (cooling water outlet from the low-temperature adsorber to lack adsorber before being sent back to the cooling tower).

3. Mathematical modeling

The equation used to describe the silica gel–water properties assumes an equilibrium process, without hysteresis, and isobaric adsorption or desorption. The modified Freundlich equation (Saha et al., 1995) below, Eq. (1), was chosen for providing a concise analytical expression of experimental data, in the form

$$q^* = A(T_S) \cdot [P_S(T_W)/P_S(T_S)]^{B(T_S)} \tag{1}$$

with

$$A(T_S) = A_0 + A_1 \cdot T_S + A_2 \cdot T_S^2 + A_3 \cdot T_S^3,$$
$$B(T_S) = B_0 + B_1 \cdot T_S + B_2 \cdot T_S^2 + B_3 \cdot T_S^3.$$

Here q^* is the refrigerant amount adsorbed in equilibrium. $P_S(T_W)$ and $P_S(T_S)$ are the saturation vapor pressure at temperatures T_W (water vapor) and T_S (silica gel). The numerical values of A_0–A_3 and B_0–B_3 are determined by least square fits to silica gel–water experimental data, which are furnished in Table 4.

3.1. Adsorption rate

The adsorption process in an adsorbent bed is considered to be controlled by macroscopic diffusion into the particle bed. The adsorption rate, dq/dt is expressed as

$$\frac{dq}{dt} = \phi(q^*, q), \tag{2}$$

where q^* is adsorption uptake at equilibrium state that can be expressed as

$$q^* = F(P, T).$$

In most of the cases equilibrium uptake is measured by the empirical equation. In the present study, q^* is measured by the same empirical equation used by Saha et al. (1995).

Table 4
Values of parameters used in Eq. (1)

Parameter	Value
A_0	31.198
A_1	−0.26650
A_2	0.769×10^{-3}
A_3	-0.73898×10^{-6}
B_0	41.581
B_1	−0.35435
B_2	0.10199×10^{-2}
B_3	-0.97034×10^{-6}

It is assumed that adsorption rate is proportional to the difference between the concentrations of equilibrium and present state. Therefore, Eq. (2) can be written as

$$\frac{\mathrm{d}q}{\mathrm{d}t} = \phi(q^*, q) = k_\mathrm{s} a_\mathrm{p}(q^* - q). \tag{3}$$

The overall mass transfer coefficient ($k_\mathrm{s}a_\mathrm{p}$) for adsorption is given by

$$k_\mathrm{s} a_\mathrm{p} = (15 D_\mathrm{s}/R_\mathrm{p}^2). \tag{4}$$

Here R_p denotes the average radius of a silica gel particle. The surface diffusivity D_s is expressed as

$$D_\mathrm{s} = D_\mathrm{so} \cdot \exp(-E_\mathrm{a}/RT). \tag{5}$$

Here D_so is a pre-exponential term that is taken as 2.54×10^{-4} m^2/s, E_a denotes activation energy, R denotes gas constant and T stands for temperature. During operation, the evaporated refrigerant would nearly simultaneously reach all the silica gel in the adsorber. In such a case, the interparticle resistance approaches to zero and modeling the adsorption/desorption rate for the silica gel–water pair in Eq. (3) is justified.

3.2. Mass balance

The mass balance of refrigerant (water) is written by neglecting the gas phase as

$$\frac{\mathrm{d}W_\mathrm{W}}{\mathrm{d}t} + W_\mathrm{S}\left(\frac{\mathrm{d}q_\mathrm{des}}{\mathrm{d}t} + \frac{\mathrm{d}q_\mathrm{ads}}{\mathrm{d}t}\right) = 0, \tag{6}$$

where W_S is the weight of silica gel packed in each of the sorption elements and W_W is the weight of refrigerant in the liquid phase. The subscripts des and ads denote respectively, desorption and adsorption.

3.3. Adsorption and desorption energy balances

Neglecting the dependence of specific heats on temperature and of adsorption heat on concentration the adsorption and desorption energy balances are described by

$$T_\mathrm{waterOUT} = T_\mathrm{ad} + (T_\mathrm{waterIN} - T_\mathrm{ad}) \cdot \exp\left(\frac{-U_\mathrm{ad} \cdot A_\mathrm{ad}}{m_\mathrm{water} \cdot C_{p\mathrm{water}}}\right), \tag{7}$$

$$\begin{aligned}&\frac{\mathrm{d}}{\mathrm{d}t}\{W_\mathrm{s}(C_{p_\mathrm{s}} + C_{p_\mathrm{w}} \cdot q) + (C_{\mathrm{pCu}} \cdot W_\mathrm{kHex} + C_{p_\mathrm{Al}} \cdot W_\mathrm{fHex})\} \cdot T_\mathrm{ad} \\ &\quad = Q_\mathrm{st} \cdot W_\mathrm{s}\frac{\mathrm{d}q}{\mathrm{d}t} + m_\mathrm{water} \cdot C_{p\mathrm{water}} \cdot (T_\mathrm{waterIN} - T_\mathrm{waterOUT}) - \delta \cdot W_\mathrm{s} \cdot C_{p_\mathrm{v} \cdot (T_\mathrm{ad} - T_\mathrm{eva})}\frac{\mathrm{d}q}{\mathrm{d}t},\end{aligned} \tag{8}$$

where

$$\delta = \begin{cases} 1, & \text{if the bed is in adsorption mode,} \\ 0, & \text{if the bed is in desorption mode.} \end{cases}$$

The subscripts IN and OUT denote respectively, inlet and outlet. For adsorption energy balances, the subscripts water and ad denote cooling water and adsorber, respectively; for desorption, they denote hot water and desorber, respectively.

Eq. (7) expresses the importance of heat transfer parameters, namely heat transfer area, A_{ad} and overall heat transfer coefficient, U_{ad}. The left hand side of the adsorber/desorber energy balance equation (Eq. (8)) provides the amount of sensible heat required to cool or heat the adsorbent (s), the water (w) as well as heat transfer tube (Cu) and fin (Al) parts of the sorption element during adsorption and desorption. The first term on the right hand side of Eq. (8) represents the release of adsorption heat during adsorption process or the input of desorption heat during desorption operation. The second term on the right hand side of Eq. (8) indicates the total amount of heat released to the cooling water upon adsorption or provided by the hot water for desorption. The last term accounts for the amount of heat needed to superheat the incoming refrigerant vapor from the evaporation temperature (T_{eva}) to adsorption temperature (T_{ads}). Eq. (8) does not account for external heat losses to the environment. However, since sensible heat output from or input to the adsorbent and metal of the adsorber/desorber heat exchanger is considered for adsorption and desorption process, respectively. That is the irreversible heat losses internal to the cycle are included in the energy balance equation.

3.4. Evaporator and condenser energy balances

For the energy balances in the evaporator and condenser, the following expression are used:

$$T_{\text{waterOUT}} = T_{ad} + (T_{\text{waterIN}} - T_{ad}) \cdot \exp\left(\frac{-U_{\text{eva,cond}} \cdot A_{\text{eva,cond}}}{m_{\text{water}} \cdot C_{p_{\text{water}}}}\right), \tag{9}$$

$$\frac{d}{dt}\{(C_{p_w} \cdot W_{ew} + C_{p_{Cu}} \cdot W_{\text{eva,cond}}) \cdot T_{\text{eva,cond}}\} = -L_w \cdot W_s \frac{dq_{des}}{dt} + m_{\text{water}} \cdot C_{p_{\text{water}}} \cdot (T_{\text{waterIN}} - T_{\text{waterOUT}}) + C_{p_{\text{water,v}}} \cdot W_s \frac{dq_{des}}{dt} \times (T_{\text{cond,des}} - T_{\text{eva,cond}}). \tag{10}$$

The subscripts water and eva denote chilled water and evaporator, respectively, for the evaporator heat balances. For the condenser heat balances, they denote cooling water and condenser, respectively. The subscripts v and ew denote water in vapor phase and the amount of liquid refrigerant inside the evaporator, respectively. For condenser energy balance the value of ew is taken as zero.

3.5. COP, cooling capacity (Q_{chill}) and waste heat recovery efficiency, η

The COP and cooling capacity (Q_{chill}) are defined by the following equations:

$$\text{COP} = \frac{Q_{chill}}{Q_{hot}}, \tag{11}$$

where

$$Q_{\text{chill}} = m_{\text{chill}} \cdot C_{p_{\text{chill}}} \cdot \int_0^{t_{\text{cycle}}} (T_{\text{chillIN}} - T_{\text{chillOUT}}) \mathrm{d}t \tag{12}$$

and

$$Q_{\text{hot}} = m_{\text{hot}} \cdot C_{p_{\text{hot}}} \cdot \int_0^{t_{\text{cycle}}} (T_{\text{hotIN}} - T_{\text{hotOUT}}) \mathrm{d}t. \tag{13}$$

The waste heat recovery efficiency, η is defined as

$$\eta = \frac{Q_{\text{chill}}}{m_{\text{water}} \cdot C_{p_{\text{water}}} \cdot \int_0^{t_{\text{cycle}}} (T_{\text{hotIN}} - T_{\text{coolIN}}) \mathrm{d}t}. \tag{14}$$

Here t_{cycle} denotes the cycle time.

3.6. Simulation procedure

The system of differential equations (2)–(10) was solved simultaneously by numerical integration using finite difference substitution in the derivatives. The data obtained from the solution process is taken from the cyclical steady state conditions of the chiller. A real chiller starts it operation with unbalanced conditions, however, after few cycles; it reaches its cyclical steady state condition. Therefore, iteration process is employed in solution procedure to fix the all initial values for the cyclical steady state conditions. In the beginning of the solution process, initial values are assumed and finally those are adjusted by the iteration process. Once the satisfactory convergence criterion is achieved, then the process goes for the next time step. The calculations were made with a time interval of 1 s. The convergence criteria is taken as 10^{-3}.

4. Results and discussion

4.1. Temperature profiles of the heat transfer fluids

Fig. 2(a) shows inlet and outlet temperature profiles of hot, cooling and chilled water obtained for the rated conditions listed in Table 3. After 250 s, the hot water outlet temperature approaches the inlet temperature value (80 °C); from this time onward there is practically no more consumption of driving heat. This led the authors to select the standard adsorption/desorption cycle time as 300 s. But the cooling water outlet temperature from the adsorber after 300 s is still 2 °C higher than its respective inlet temperature. The reason for this is the increasing amount of refrigerant requiring cooling at the end of the adsorption process, in contrast to the desorption process, where little refrigerant remains to be heated. Cooling water outlet temperature gradually returns to its inlet at 30 °C confirming that condensation takes place satisfactorily in the condenser within the given adsorption/desorption cycle time. Fig. 2(b) shows a comparison between chilled water and condenser coolant outlet temperatures for two-bed and three-bed cycles. Condenser coolant outlet temperatures approach its inlet after 250 s for the both two-bed and three-bed cycles. Condenser peak temperature is slightly reduced in the case of three-bed cycle in comparison with the two-bed cycle. The delivered chilled water temperature, however, continues

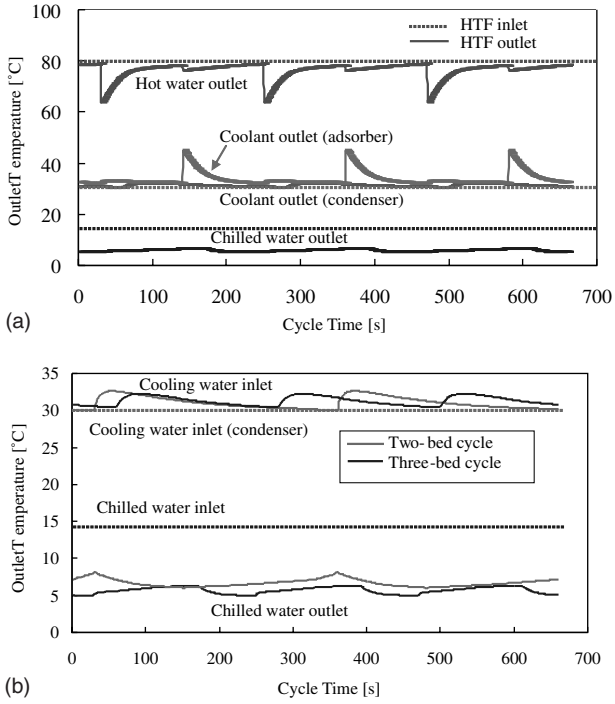

Fig. 2. (a) Outlet temperature profiles of heat transfer fluids for three-bed cycle. (b) A comparison between chilled water and condenser cooling water outlet temperatures for two-bed and three-bed adsorption systems.

below the inlet temperature in the whole cycle for the both two and three-bed cycles, showing the continuation of cooling energy production, which is highly desirable. Another noteworthy observation is that chilled water outlet temperature tends to be smoothened in the case of three-bed scheme. This may lead to the elimination of downstream cooling devices for demanding process cooling and dehumidification in case of three-bed cycle.

4.2. Operating temperatures

Fig. 3(a) and (b) show plots of simulated results of cooling capacity and COP variations with hot water inlet temperatures. Cooling capacity rises from 0.83 to 2.22 kW as the hot water inlet temperature is increased from 60 to 95 °C with a cooling water at temperature 30 °C. This is because the amount of refrigerant circulated increases, due to increased refrigerant desorption with higher driving source temperature. With hot water temperature variation, the simulated COP values peak between 80 and 90 °C. For hot water inlet temperature between 60 and 85 °C, the COP drop reflects lower cooling capacity, while between 85 and 95 °C it suggests an increase in heat losses as the sorption elements repeatedly switch between adsorption and desorption modes. The optimum COP value is 0.38 for hot water inlet temperature at 85 °C in combination with the coolant and chilled water inlet temperatures are at 30 and 14 °C, respectively. The delivered chilled water temperature is 6 °C for this operation condition.

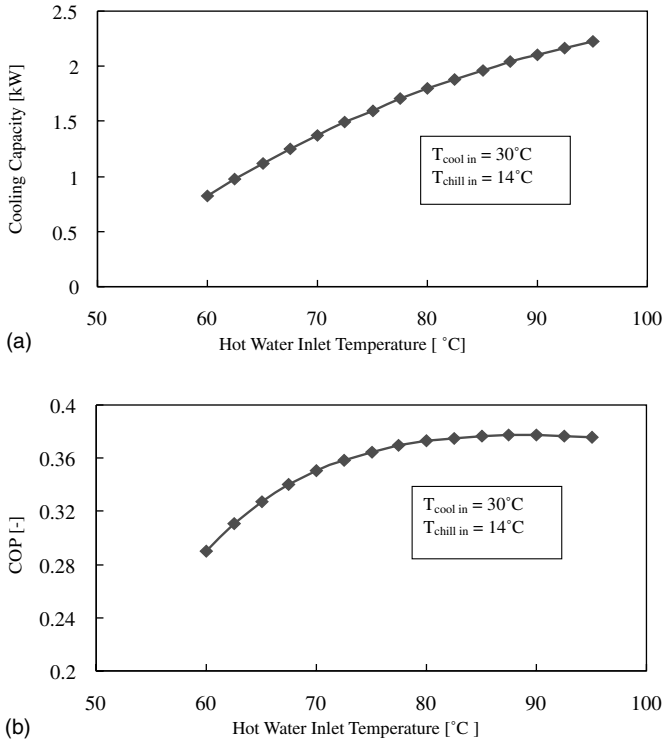

Fig. 3. Hot water temperature effect on (a) cooling capacity and (b) COP.

Fig. 4(a) and (b) show the effect of cooling water inlet temperatures on cooling capacity and COP. In the present simulation, cooling water mass flow rate into each adsorber is taken as 0.192 kg/s, while for the condenser the coolant mass flow rate is taken as 0.332 kg/s. The cooling capacity increases steadily as the cooling water inlet temperature is lowered from 35 to 20 °C. This is due to the fact that lower adsorption temperatures result in larger amounts of refrigerant being adsorbed and desorbed during each cycle. The simulated COP values also increase with lower cooling water inlet temperature. For the three-bed chiller the COP value reaches 0.43 with 80 °C driving source temperature in combination with a coolant temperature of 22 °C.

4.3. Adsorption/desorption cycle time

Simulated results of cooling capacity and COP variations with adsorption/desorption cycle time are shown in Fig. 5(a) and (b), respectively. The pre-heating or pre-cooling cycle time is considered as 30 s. The highest cooling capacity values were obtained for cycle times between 180 and 300 s. When cycle times are shorter than 180 s, there is not enough time for adsorption or desorption to occur satisfactorily. As a result, cooling capacity decreases abruptly (see Fig. 5(a)). On the other hand, when cycle times are longer than 360 s, cooling capacity decreases gradually since adsorption tends to become less intense after the first five minutes, gradually decreasing as the adsorbent approaches to its equilibrium condition. The COP increases uniformly with longer

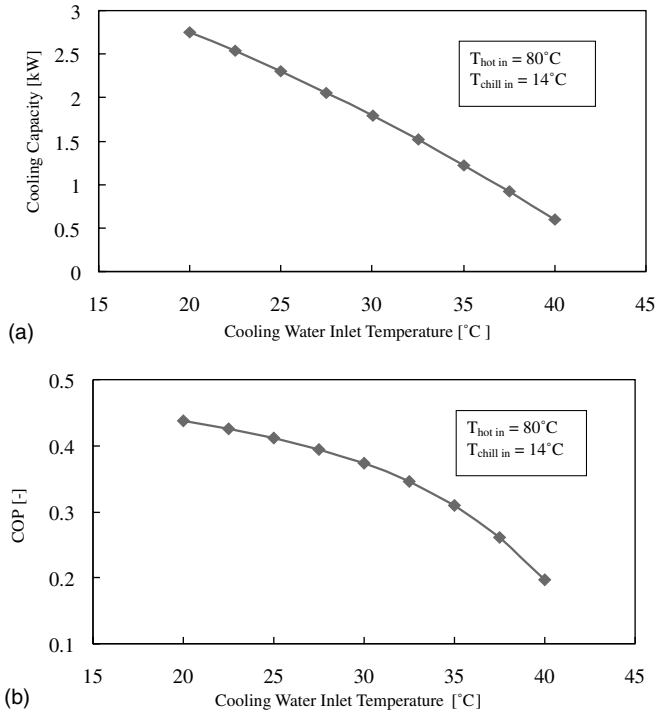

Fig. 4. Cooling water temperature effect on (a) cooling capacity and (b) COP.

adsorption/desorption cycle time (see Fig. 5(b)). This occurs because of the lower consumption of driving heat with longer cycles.

4.4. Waste heat recovery efficiency

Fig. 6 shows the waste heat recovery efficiency, η of the two-bed and three-bed adsorption cycles as a function of hot water inlet temperature. For the three-bed adsorption cycle, η rises from 0.0345 to 0.0444 as the hot water inlet temperature is increased from 60 to 85 °C with a cooling water at temperature 30 °C. This is because of the improvement in cooling capacity. For hot water inlet temperature between 85 and 95 °C, the η drop reflects lower cooling capacity. The waste heat recovery efficiency of a two-bed adsorption chiller at rated conditions (see Table 3) is 0.0396. It can be appreciated that, from two to three beds, the waste heat recovery efficiency is boosted by about 35%.

4.5. Dühring diagram

Fig. 7 depicts the cyclic-steady-state Dühring diagram of the three-bed adsorption cycle simulated from our current formalism. The adsorption/desorption cycle time and pre-heating/pre-cooling cycle time were set to 300 and 30 s respectively, which corresponds to the manufacturer's specification of the commercially available two-bed silica gel–water adsorption chiller. In Fig. 7,

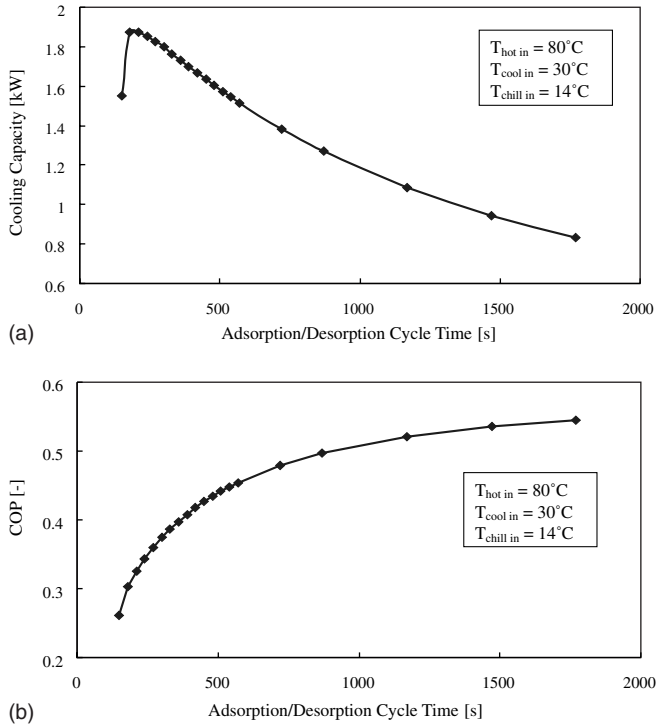

Fig. 5. Adsorption/desorption cycle time effect on (a) cooling capacity and (b) COP.

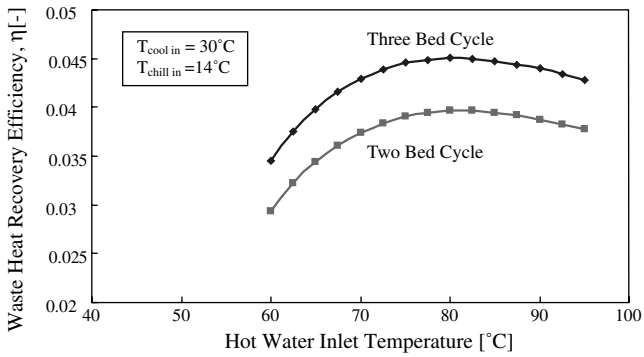

Fig. 6. A comparison between the waste heat recovery efficiency of two-bed and three-bed cycles.

the various modes of a complete cycle are designated by numbers: desorption mode (1–2), pre-cooling mode (2–3), adsorption mode (3–4) and pre-heating mode (4–1). One can observe that during the cold-to-hot thermal swing of the bed, momentary adsorption takes place at the inception even though heat source is already applied. Subsequently, the thermal swing is assumed to be dictated by the isostere (dashed line in Fig. 7). The hot-to-cold thermal swing is also assumed to be isosteric. The pre-heating/pre-cooling phase is stopped before the beds are sufficiently heated

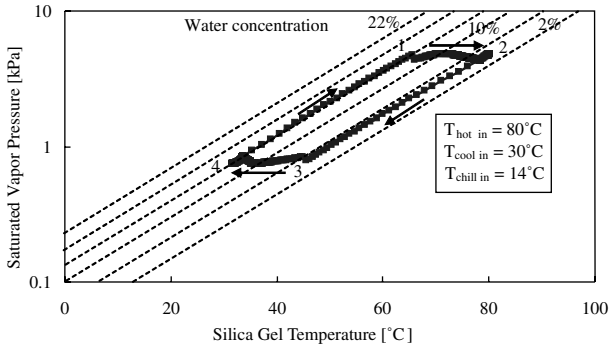

Fig. 7. Dühring diagram of three-bed adsorption chiller for rated conditions.

and cooled so that they do not reach the pressures in the condenser and evaporator. Consequently, there is a momentary period when the condensate on the condenser tube bundles is evaporated and adsorbed by the heated bed. This evaporation maintains similar pressure in the bed and condenser. Similarly, from Fig. 7 it is observed that at the end of the switching phase, there is a sudden drop in the bed pressure. This causes the adsorbate in the cool bed to momentarily desorbs and condenses into the evaporator. Another observation from the same figure is that the silica gel temperature at the end of adsorption is about 2 °C higher than the cooling water inlet temperature, and at the end of desorption the adsorbent temperature is about 1 °C lower than the hot water inlet temperature. This occurs because the sorption element must periodically switch between adsorption and desorption temperatures within the relatively short time intervals.

5. Conclusions

This paper investigates analytically the performance of an innovative silica gel–water based three-bed adsorption chiller. The main advantage in the three-bed adsorption cycle is its ability to utilize effectively low-temperature waste heat between 60 and 95 °C as the driving heat sources with a coolant at 30 °C. The three-bed chiller is operational with the heat source and heat sink temperature difference as small as 30 °C. In the case of three-bed cycle, the delivered chilled water temperature tends to be smoothened in comparison with that of two-bed cycle. This prevents a sudden temperature drop in the evaporator, reducing the risk of ice formation. This suggests that the downstream temperature smoothening device may be downsized or eliminated for the cooling application.

Cooling capacity increases with higher driving source temperature along with a fixed coolant temperature. With cooling water temperature at 30 °C, optimum COP values are obtained with driving source temperatures between 80 and 90 °C. Both cooling capacity and COP decrease with higher coolant inlet temperatures. Long adsorption/desorption cycle time results in COP gains and cooling capacity losses. Optimum cooling capacity values are obtained for adsorption–desorption cycle time between 180 and 300 s with a fixed pre-heating or pre-cooling cycle time. Waste heat recovery efficiency of the three-bed system is about 35% higher than that of the two-bed system.

The innovative three-bed adsorption chiller has a significant market potential as it can be used as the bottoming cycle of existing power generation cycles. From the above perspectives, the use of unexploited low-temperature waste heat may offer an attractive possibility for improving energy efficiency.

Acknowledgement

This work was funded by the New Energy and Industrial Technology Development Organization (NEDO) under International Joint Research Grant Proposal 01GP1.

References

Alefeld, G., Bauer, H.C., Mailer-Laxhuber, P., Rothmeyer, M., 1981. A zeolite heat pump, heat transformer and heat accumulator. In: International Conference on Energy Storage, Brighton, UK, pp. 61–72.

Beijer, H.A., Horsman, J.W.K., 1994. SWEAT thermomechanical heat pump, heat storage system. In: Proceedings of the International Absorption Heat Pump Conference, ASME-AES 31, New Orleans, USA, pp. 457–462.

Boelman, E., Saha, B.B., Kashiwagi, T., 1995. Experimental investigation of a silica gel–water adsorption refrigeration cycle—the influence of operating conditions on cooling output and COP. ASHRAE Trans. 101, 358–366.

Chua, H.T., Ng, K.C., Malek, A., Kashiwagi, T., Akisawa, A., Saha, B.B., 1999. Modeling and performance of two-bed, silica gel–water adsorption chiller. Int. J. Refrigeration 22, 194–204.

Chua, H.T., Ng, K.C., Malek, A., Kashiwagi, T., Akisawa, A., Saha, B.B., 2001. Multi-bed regenerative adsorption chiller—improving the utilization of waste heat and reducing the chilled water outlet temperature fluctuation. Int. J. Refrigeration 24, 124–136.

Douss, N., Meunier, F., 1989. Experimental study of cascading adsorption cycles. Chem. Eng. Sci. 44, 225–235.

Exell, R.H.B., Bhattacharya, S.C., Upadhyaya, Y.R., 1993. Research and development of solar powered desiccant refrigeration for cold storage application. Asian Institute of Technology, Bangkok, AIT Research Report No. 265.

Guilleminot, J.J., Chalfen, J.B., Choisier, A., 1994. Heat and mass transfer characteristics of composites for adsorption heat pumps. In: Proceedings of the International Absorption Heat Pump Conference, ASME-AES 31, New Orleans, USA, pp. 401–406.

Klein, H.P., Willers, E., Groll, M., 2000. Thermally driven high performance sorption heat pumps. In: Proceedings of Symposium on Energy Engineering 3, Hong Kong, pp. 1130–1137.

Pons, M., Guilleminot, J.J., 1986. Design of an experimental solar-powered, solid-adsorption ice maker. Trans. ASME J. Solar Energy Eng. 108, 332–337.

Saha, B.B., Kashiwagi, T., 1997. Experimental investigation of an advanced adsorption refrigeration cycle. ASHRAE Trans. 103, 50–58.

Saha, B.B., Boelman, E., Kashiwagi, T., 1995. Computer simulation of a silica gel–water adsorption refrigeration cycle—the influence of operating conditions on cooling output and COP. ASHRAE Trans. 101, 348–357.

Tamainot-Telto, Z., Critoph, R.E., 2001. Monolithic carbon for sorption refrigeration and heat pump application. Applied Thermal Eng. 21, 37–52.

Tchernev, D.I., 1979. Solar air conditioning and refrigeration systems utilizing zeolites. In: Proceedings of the Meetings of Commissions E1-E2, Jerusalem, pp. 209–215.